 doi:10.20944/preprints202101.0064.v1

Effect of Pr_6O_{11} on the Microstructures and Mechanical Properties of High-Strength Steel Weld Metal

Tianli Zhang [1,2,*], Hang Yu [1], Shiliang Li [3], Weiguang Wang [1], Wen Wu [1], Haoxin Chen [1] and Yu Chen [1]

[1] School of Materials Engineering, Shanghai University of Engineering Science, Shanghai 201620, China; 2582249607@qq.com (H.Y.); 1457958357@qq.com (W.G.W.); 2633857371@qq.com (W.W.); 305834390@qq.com (H.X.C.); yahwehchen@qq.com (Y.C.)

[2] Shanghai Collaborative Innovation Center of Laser Advanced Manufacturing Technology, Shanghai 201620, China

[3] Shaanxi Tyon Intelligent Remanufacturing Co.,Ltd, Xi'an 710016, China; glishiliang@163.com (S.L.L.)

* Correspondence: zhangtianli925@163.com (Z.T.L.); Tel.: +86 21 67791474

Abstract: The effect of Pr_6O_{11} on the microstructure and mechanical properties of high-strength steel weld metal was investigated by optical microscopy, scanning electron microscopy and mechanical testing. Three different contents of Pr_6O_{11} were added to the flux-cored wires. The results demonstrate that the addition of 1% Pr_6O_{11} can promote the refinement and spheroidization of inclusions, refine the grains, form acicular ferrites in the weld metal, and significantly improve the toughness. The addition of Pr_6O_{11} promoted the formation of rare earth composite inclusions and acicular ferrites in the weld metal, refined the lath microstructure, inhibited the formation of martensite and bainite. The crack formation mode changed from the boundary cracking of the bainite clusters caused by the surface shear stress to the surface shear stress-induced decohesion of inclusion. Excessive addition of Pr_6O_{11} will reduce the number of inclusion nucleation and deteriorate the mechanical properties. The wire No.2 with 1% Pr_6O_{11} had the good comprehensive mechanical properties.

Key words: high-strength steel; weld metal; Pr_6O_{11}; microstructure; mechanical properties

1. Introduction

The attainment of both strength and toughness is a vital requirement for most structural materials; unfortunately these properties are mutually exclusive [1]. Improving the toughness of high-strength steel weld metal is a hot spot in welding field. Alloying elements are one of the main factors that control the weld metal microstructure and mechanical properties. Therefore, with the development of high-strength steels, the research and development of micro-alloying welding consumables, and the study of the influence of microalloying elements on the microstructure and properties of welds and heat-affected zones are the hot spots in the field of welding. The volume fractions of acicular ferrites (AF) were decreased as boron contents increased from 32 to 103 ppm in high-strength steel welds. The upper bainite was formed in the weld metal with 103 ppm boron wire, while was not formed in the weld metal with the wire of 32 ppm and 60 ppm boron contents [2]. Effect of Zr on the chemical component and size distribution of Ti-bearing inclusions, favored the grain refinement of the welding induced, coarse-grained heat affected zone with enhanced impact toughness in Ti-killed steels [3]. In order to enhance the toughness of weld metal, the optimum Ti content of the welded metal in the HSLA steel should be around

Preprints (www.preprints.org) | NOT PEER-REVIEWED | Posted: 4 January 2021 doi:10.20944/preprints202101.0064.v1

of 150 ppm. However, this amount also depends on the content of other alloying elements because the AF formation is influenced simultaneously by the proper combination of alloying elements [4]. the amount of AF in Ti-B-N system is controlled by the balance between BN as an energetically favourable site for AF nucleation and soluble boron which acts as a hardenability element suppressing grain boundary ferrite formation [5].

Many research has been done on the microstructure transformation of weld metals and mainly focused on the micro-alloys, such as Ti and Zr [6-8]. However, there have been few, if any, studies on the effect of rare earth elements on the strength and toughness of high-strength steel weld metal. Therefore, rare earth oxide is the research object in this paper, and we conduct a systematic study on the effect of Pr_6O_{11} on the microstructures and mechanical properties of high-strength steel weld metal.

2. Experimental procedure

The flux-cored wire has the advantage of strong adaptability. It is very convenient and easy to adjust the proportion and composition of powder in the flux, and can provide the chemical composition required by the weld. Therefore, the flux-cored wire is used in this experiment. The purity of Pr_6O_{11} was 99.99%. To study the effect of Pr_6O_{11} on microstructures and mechanical properties of weld metal, three different contents of Pr_6O_{11} were added to the flux-cored wires: wire No.2, wire No.3 and wire No.4 were added to 1%, 2%, and 3% Pr_6O_{11}, respectively, and wire No.1 (Pr_6O_{11} 0%) was the control group. The weld metals were prepared by welding according to the AWS standard A5.29/A5.29M [9]. The pass arrangement and welding parameters are shown in Figure 1a and Table 1, respectively. The base metal plates were Q235 steel. The reason for selecting Q235 steel is that it is readily available and does not have much alloying elements to add to those in the weld metal. Furthermore, the groove faces and the contacting face of the backing steel of each weld were first buttered no less than two layers using the wire to be used for subsequent welding. Then, the buttered faces were cut down to 3 mm thick at an angle of 22.5°. The preheat and interpass temperature was measured by a digital non-contact laser infrared thermometer gun at the location shown in Figure 1a. After each welding pass, the assembly was cooled in still air at room temperature to 150–160°C without special control of cooling or post-weld heat treating. The specimens were prepared according to AWS standards A5.29/A5.29M [9] and B4.0 [10]. The groove weld test assembly for mechanical properties is schematically shown in Figure 1a. The round tensile specimens and Charpy V-notch impact specimens are shown in Figures 1b and 1c. After preparing the standard specimens, the mechanical properties of the weld metal were tested with a WAW-6000 tensile test machine, and the yield strength, tensile strength and elongation were recorded. The Charpy V-notch impact test was performed by an JB30B impact testing machine after the impact specimens were cooled to -40°C. The chemical compositions of weld metals were determined with a Q4 optical emission spectrometer. Metallographic specimens were prepared and etched with 4% natal. The microstructure of the weld metal was observed using optical microscopy, and the proportion of the microstructure was calculated. The Vickers hardness of the weld metal was measured using a HXD-1000TMSC/LCD Vickers hardness tester. The fracture surfaces were examined by scanning electron microscopy (SEM) with a Tescan Vega3 microscope, and the inclusions in the dimples were analyzed by energy dispersive spectrometry (EDS).

Preprints (www.preprints.org) | NOT PEER-REVIEWED | Posted: 4 January 2021 doi:10.20944/preprints202101.0064.v1

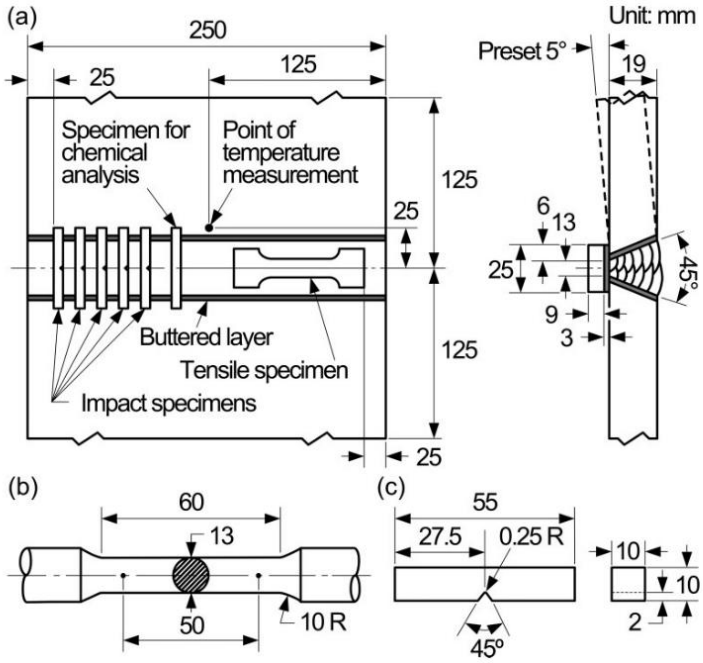

Figure 1. Groove weld test assembly for mechanical properties: (a) test plate showing location of test specimens; (b) dimensions of round tensile specimen; (c) dimensions of Charpy V-notch impact specimen.

Table 1. Welding parameters used in experiments.

Voltage (V)	Current (A)	Wire stick-out (mm)	Welding speed (cm ·mm^{-2})	Shielding gas (%)	Heat input (kJ·mm^{-2})	Preheat/interpass temperature (℃)
29-31	220-240	15-20	250-260	80Ar+20CO_2	1.67-1.81	150-160

3. Results and discussion

3.1. Microstructure and mechanical properties of weld metals

The chemical compositions and mechanical properties of the weld metals are shown in Table 2 and Figure 2, respectively. Figure 2 illustrates the tensile strength and yield strength curves of the weld metals with the addition of various Pr_6O_{11} contents. With the addition of Pr_6O_{11} from 0% to 3%, the strength of weld metal gradually decreased. With the addition of 1% Pr_6O_{11}, the tensile strength of the weld metal decreased from the initial value of 843 MPa to 835 MPa, and the yield strength decreased from 793 MPa to 740 MPa. With the addition of 3% Pr_6O_{11}, the weld metal obtained the lowest strength with a tensile strength of 809 MPa and a yield strength of 700 MPa. The yield strength of weld metal decreased significantly with the addition of Pr_6O_{11}, while the tensile strength of weld metal decreased slightly with the addition of Pr_6O_{11}. The low-temperature impact toughness of the weld metal is shown in Figure 2. With the gradual increase in Pr_6O_{11}, the low-temperature impact toughness of the weld metals obviously increased, and the low-temperature impact toughness of the weld metal increased first and then decreased. The impact value of wire No.2 with 1% Pr_6O_{11} was the highest, which was 70 J. The low-temperature impact toughness of the weld metal with 3% Pr_6O_{11} added is basically the same as that of the weld metal without Pr_6O_{11}, and the strength of weld metal decreased. The addition of excessive Pr_6O_{11} cannot

Preprints (www.preprints.org) | NOT PEER-REVIEWED | Posted: 4 January 2021 doi:10.20944/preprints202101.0064.v1

improve the low-temperature impact toughness of the weld metal.

Table 2. Results of chemical compositions of weld metals.

Wire No.	Chemical compositions (wt%)							
	C	Mn	Si	P	S	Cr	Ni	Mo
1 (0%Pr6O11)	0.038	1.891	0.424	0.013	0.0076	0.405	2.122	0.625
2 (1%Pr6O11)	0.049	2.182	0.533	0.012	0.0075	0.492	2.258	0.882
3 (2%Pr6O11)	0.046	2.016	0.520	0.013	0.0076	0.462	2.060	0.872
4 (3%Pr6O11)	0.041	2.024	0.450	0.013	0.0078	0.484	2.254	0.714

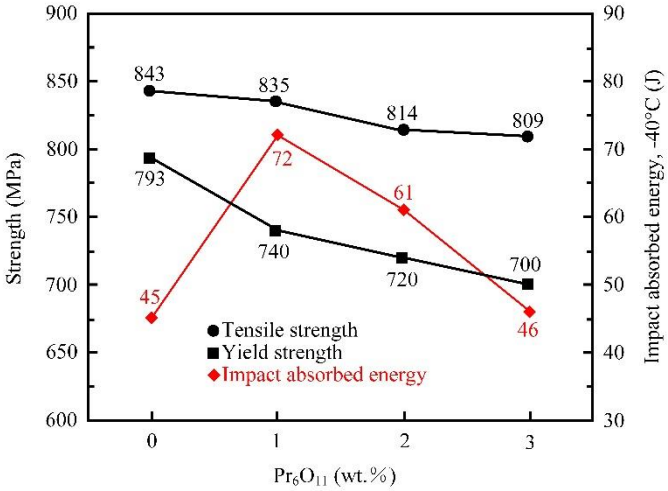

Figure 2. Effects of Pr_6O_{11} on the strength and impact absorbed energy of weld metals.

The Vickers hardness and elongation of the weld metals are shown in Figure 3. Wire No.1 with 0% Pr_6O_{11} had the highest Vickers hardness, which was 252 Hv. Wire No.4 with 3% Pr_6O_{11} had the lowest Vickers hardness, which was 235 Hv. With the addition of 2% Pr_6O_{11}, the Vickers hardness value of the weld metal had a large dispersion, which indicates that the microstructure of the weld metal was not uniform. With the addition of 3% Pr_6O_{11}, the dispersion of the weld metal Vickers hardness value was the smallest, which indicates that the weld metal microstructure was uniform. Wire No.1 with 0% Y_2O_3 had the lowest elongation, which was 17%. Wire No.4 with 3% Y_2O_3 had the highest elongation, which was 21%.

Preprints (www.preprints.org) | NOT PEER-REVIEWED | Posted: 4 January 2021 doi:10.20944/preprints202101.0064.v1

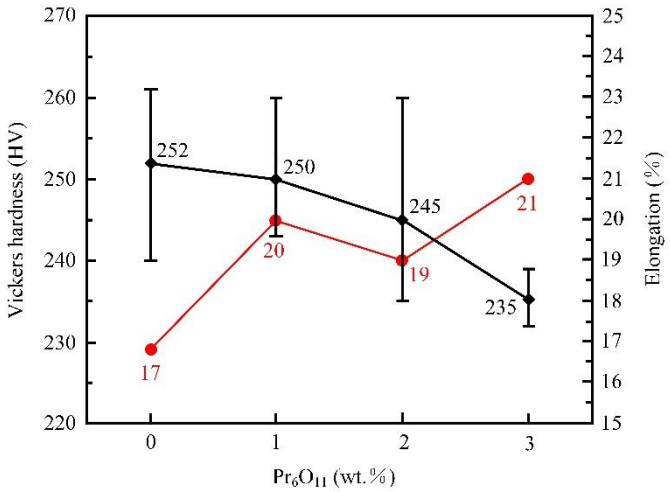

Figure 3. Effects of Pr_6O_{11} on the Vickers hardness and elongation of weld metals.

The microstructure quantitative statistical analysis and microstructure of the weld metals with different Pr_6O_{11} contents are shown in Table 3 and Figure 4. With the addition of Pr_6O_{11}, the AF of the weld metal increased first and then decreased, the granular bainite (GB) and degenerate upper bainite (DUB) of the weld metal decreased first and then increased. When the amount of Pr_6O_{11} added was 1%, the content of AF in the weld metal was the highest, which was 61%, and the content of GB and DUB was the lowest. which were 26% and 10%, respectively. The addition of Pr_6O_{11} promoted the nucleation and growth of AF, and the microstructure in the weld metals was gradually refined. Without Pr_6O_{11} added, the lath structure of the weld metal was relatively coarser, as shown in Figures 4a and e. With the addition of 1% Pr_6O_{11}, the weld metal was composed of GB, DUB and AF, the block microstructure and lath microstructure were reduced, and the microstructure was obviously refined, as shown in Figures 4b and f. With further addition of Pr_6O_{11}, the nucleation of GB and DUB increased, the AF content decreased, and the grain of weld metal become coarser, as shown in Figures 4c and g. With the addition of 3% Pr_6O_{11}, the unevenness of the microstructure was serious and the lath microstructure increased, as shown in Figures 5d and h. It can be clearly seen that the addition of 1% Pr_6O_{11} can refine the grains, form AF in the weld metals. With the excessive addition of Pr_6O_{11}, the formation of bainite was promoted, and the low-temperature impact toughness of the weld metal decreased. Excessive addition of Pr_6O_{11} was not conducive to the improvement of the toughness of the weld metal, and the micrograph was consistent with the impact absorbed energy curve of the weld metal.

Table 3. Results of quantitative statistical analysis of microstructures in weld metals.

Wire No.	**Area fraction%**			
	Acicular ferrite	**Martensite**	**Granular bainite**	**Degenerate upper bainite**
1 (0%Pr6O11)	32	15	28	25
2 (1%Pr6O11)	61	3	26	10
3 (2%Pr6O11)	56	3	29	12
4 (3%Pr6O11)	38	4	34	24

Preprints (www.preprints.org) | NOT PEER-REVIEWED | Posted: 4 January 2021 doi:10.20944/preprints202101.0064.v1

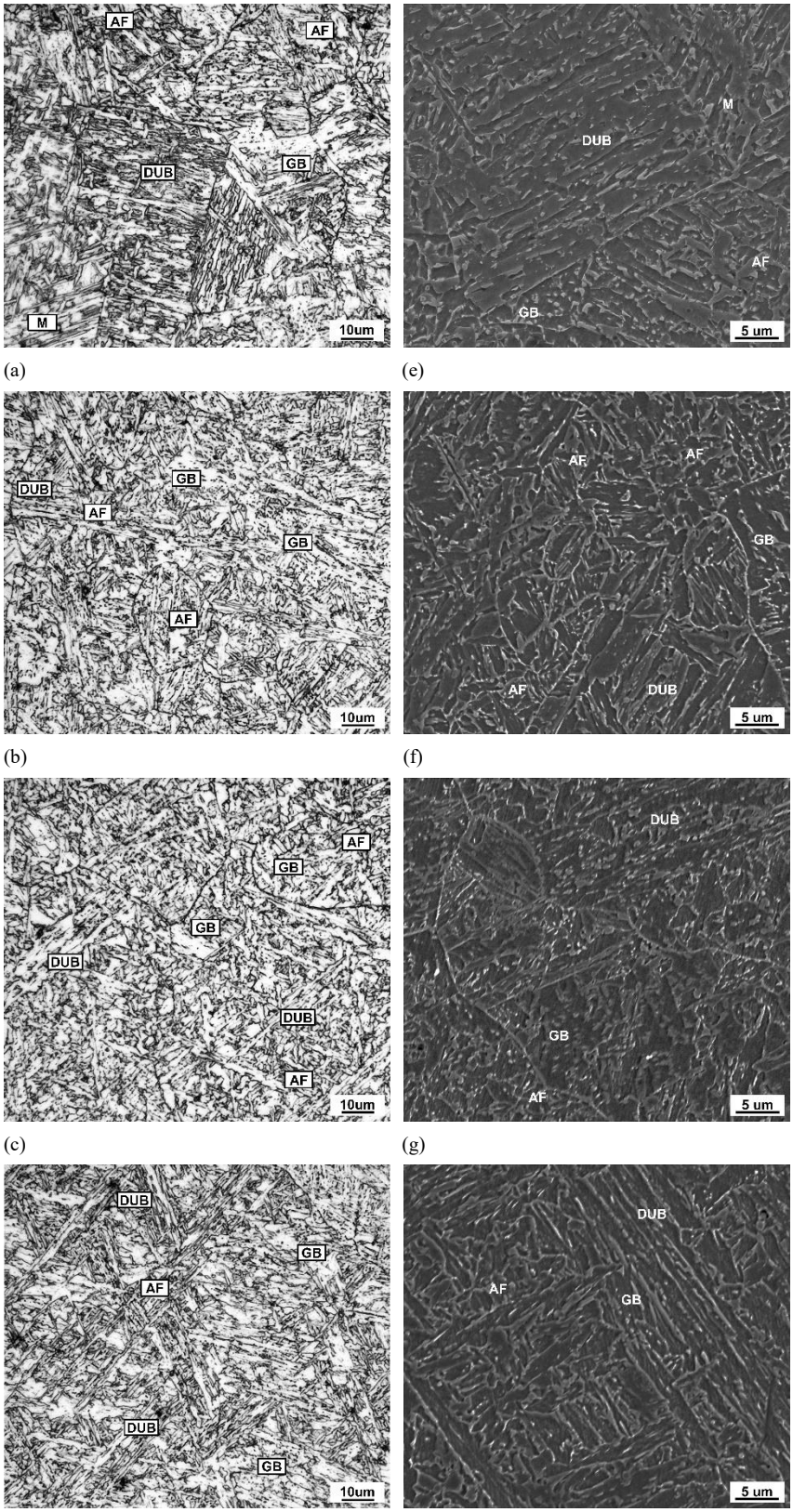

Figure 4. Micrographs of weld metals: (a) and (e) wire No.1; (b) and (f) wire No.2; (c) and (g) wire No.3; (d) and (h) wire No.4.

Preprints (www.preprints.org) | NOT PEER-REVIEWED | Posted: 4 January 2021 doi:10.20944/preprints202101.0064.v1

The addition of Pr_6O_{11} can promote the formation of AF in the weld metal. The rare-earth elements can both spheroidize and refine inclusions because they usually enrich at inclusions in weld metal deposits [11]. For liquid metals, the new inclusion phases in spherical forms normally have the maximum surface tension under the premise of the same volume. This is mainly ascribed to the fact that spherical inclusions have the minimum thermodynamic driving force during its growing process in weld pool. On the other hand, the amount of inclusions can be enhanced by the rare-earth elements, which accordingly provides more nucleation positions for AF [11, 12]. AF is considered an excellent microstructure component to improve the toughness through effective grain refinement, and AF grains can divide large austenite grains into fine individual regions to form a mixed microstructure of fine particles [13, 14, 15]. The AF microstructure has a large-angle grain boundary, which can effectively increase the crack extension path during fracture. The increase in energy required for crack extension helps improve the low-temperature impact toughness of the weld metal, which can explain the higher impact energy of wire No.2 than those of wire No.1. the addition of Pr_6O_{11} can be used as the core of AF heterogeneous nucleation, the grain core preferentially attaches to the surface of these impurities and promotes the formation of a large amount of AF, and the formation of a large AF content inhibits the formation of Martensite, B and other phases. Martensite and DUB are the main strengthening phases, which can improve the strength and hardness of the weld metal. AF and GB are toughening phases in the weld metal that mainly improve the low-temperature impact toughness of the weld metal [16]. The formation of AF causes a decrease in Martensite and DUB strengthening phases in the weld metal, so addition of Pr_6O_{11} can cause a decrease in strength and an increase in toughness. As the content of Pr_6O_{11} excesses 1%, the inhibition behavior of the nucleation of GB and DUB was revitalized. The difference in the electronegativity between Pr and Fe is very large, which is not conducive to the formation of solid solution in the weld metal. The Pr will preferentially segregate in inclusions [17]. Excessive addition of Pr_6O_{11} can increase the lath structure of the weld metal and lead to the coarsened grain. This is mainly ascribed to the fact that excessive addition of Pr_6O_{11} leads to grain boundary segregation of Pr_6O_{11}, causing grain boundary contamination. The segregation of Pr in the grain boundaries and nearby areas reduces the system energy to a metastable state, which is thermodynamically beneficial [17].

3.2. Fracture morphology of weld metals

The fractures of different Charpy V specimens at -40°C are shown in Figure 5. With the addition of Pr_6O_{11}, the fracture mode changed from quasi-cleavage fracture to ductile fracture with dimples, the tear ridges were scattered between the cleavage fracture and the dimple, the width of the dimples decreased, the depth of the dimples increased, and the distribution of the dimples was even. Dimples could improve the low-temperature impact toughness of the weld metals, which is consistent with the low-temperature impact curve in Figure 2. Without Pr_6O_{11}, the dimples had the largest width and smallest depth, and the distribution of dimples was extremely uneven and concentrated in a few areas, which shows that the energy absorbed was low and the toughness was poor, as shown in Figure 5a. With the increase in Pr_6O_{11}, the dimple width in the fracture of the specimen decreased, the depth increased, and the distribution was more uniform, as shown in Figure 5b. With the addition of 1% Pr_6O_{11}, the number of dimples in the fracture reached the maximum, the dimples were narrow and deepest, and the distribution was the most uniform. With the increase in Pr_6O_{11}, the dimple width in the fracture of the specimen increased, the depth decreased, as shown in Figures 5c and d. There were inclusions in dimples that promoted the nucleation of AF, and wire No.1 had the fewest inclusions, as shown in Figure 5a. With the addition of 1% Pr_6O_{11}, the number of inclusions increased, and the inclusions were significantly refined, there were

Preprints (www.preprints.org) | NOT PEER-REVIEWED | Posted: 4 January 2021 doi:10.20944/preprints202101.0064.v1

the most inclusions, and the distribution of inclusions was the most uniform, as shown in Figure 5b. The area of cleavage fracture where the crack source was located in wire No.1 was the largest, and the river pattern was smooth and continuous. The cracks started from between the B clusters and propagated along the adjacent B clusters, and the arrow direction was the crack propagation direction, as shown in Figure 5e, which is consistent with the micrograph in Figures 4a and e. The crack source generated by the decohesion of an inclusion, and the pit after the inclusion fell off appeared at the crack source, as shown in Figure 5f. When the Pr_6O_{11} content increased from 0% to 3%, the average area of the cleavage fracture where the crack source was located gradually decreased first and increased, the river pattern gradually decreased first and increased, the crack source in wire No.2 had the smallest average area and smallest river pattern, as shown in Figures 5e, f, g and h. It can be seen that the river pattern in the weld metal of wire No.1 and wire No.4 is smooth and continuous, which indicates that the crack propagation resistance is low and the crack is easy to expand, resulting in a decrease in the low-temperature impact toughness of the weld metal.

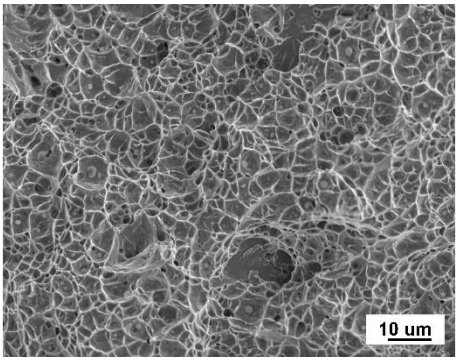

(a)

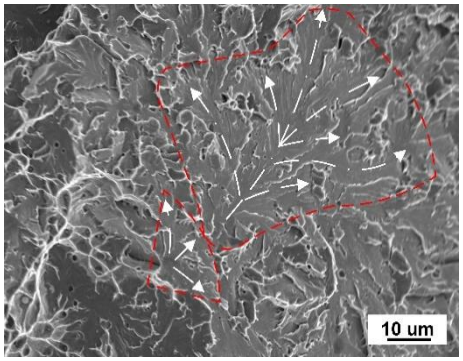

(e)

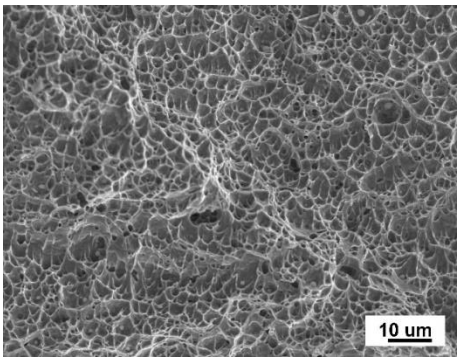

(b)

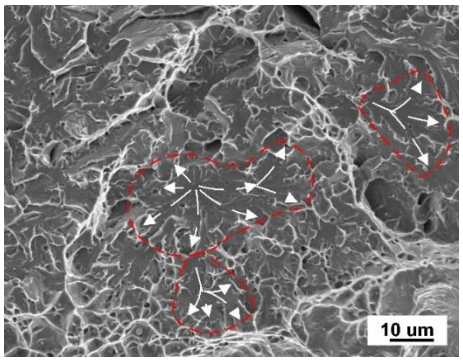

(f)

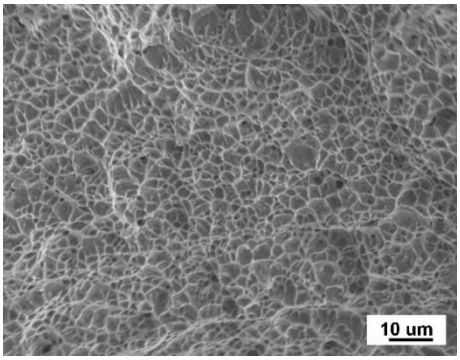

(c)

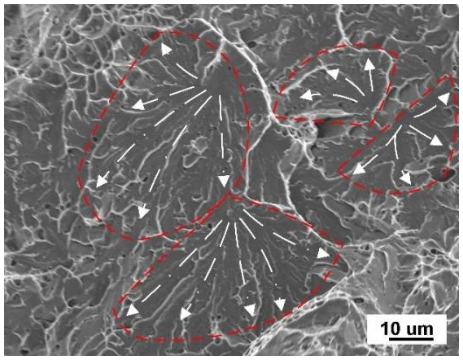

(g)

Preprints (www.preprints.org) | NOT PEER-REVIEWED | Posted: 4 January 2021 doi:10.20944/preprints202101.0064.v1

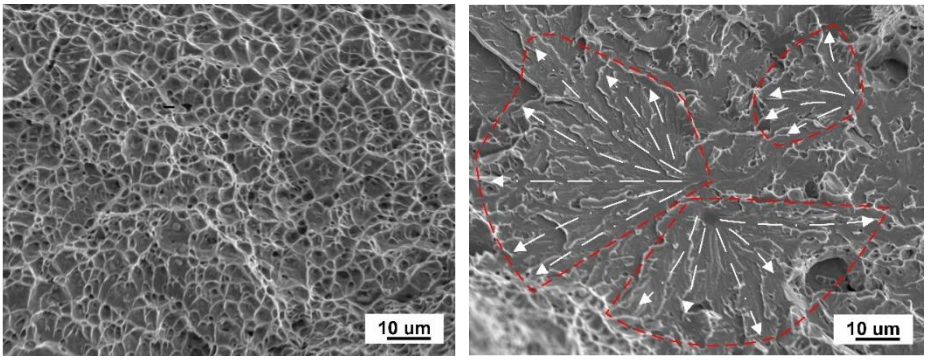

(d) (h)

Figure 5. SEM images of dimples and cleavage facets in weld metals:
(a) and (e) wire No.1; (b) and (f) wire No.2; (c) and (g) wire No.3; (d) and (h) wire No.4.

Figure 6 shows the EDS of inclusions on the fracture surface. The inclusions in dimples were basically spherical. When Pr_6O_{11} was not added, the EDS analysis indicates that the inclusions were mainly composed of Fe and a small amount of Al, Si, Zr and Ti. When 1% Pr_6O_{11} was added, the O content in the inclusions increased significantly, and Pr was found in the inclusions. It can be seen that with the addition of Pr_6O_{11}, the Fe in inclusions gradually decreased. When Pr_6O_{11} was not added, the inclusion composition was mainly Al-O, Ti-O and Zr-O composite inclusions. Al and Zr provided a large number of nucleating cores for Ti oxide. After the inclusions nucleate, they absorb the surrounding Mn and Si and continue to grow [18, 19]. With the addition of Pr_6O_{11}, Pr_6O_{11} promoted the formation of inclusions and combined with Al, O, Ti and other elements to form rare earth composite inclusions. The presence of complex inclusions containing Ti and Ca has been associated with a higher inclusion/matrix interface disregistry which increases the ferrite nucleation potential of the inclusions [20]. Therefore, rare earth composite inclusions were more conducive to the spheroidization and refinement of inclusions, and promote the formation of AF. With the excessive addition of Pr_6O_{11}, the contents of Fe, Pr, Ti and Ca in the inclusions all decreased. This indicates that the decrease of inclusion in the weld metal was caused by the decrease of Pr and Fe content in the inclusion, which leads to the decrease of the content of Ti and Ca in the inclusions and the decrease of the nucleation number of AF. Fe was essential for the nucleation of inclusions, even if rare earth elements existed in the inclusions. the obvious reduction of low-temperature toughness of the weld metals was owed to the decrement of nucleation rate of AF as a result of inappropriate inclusions.

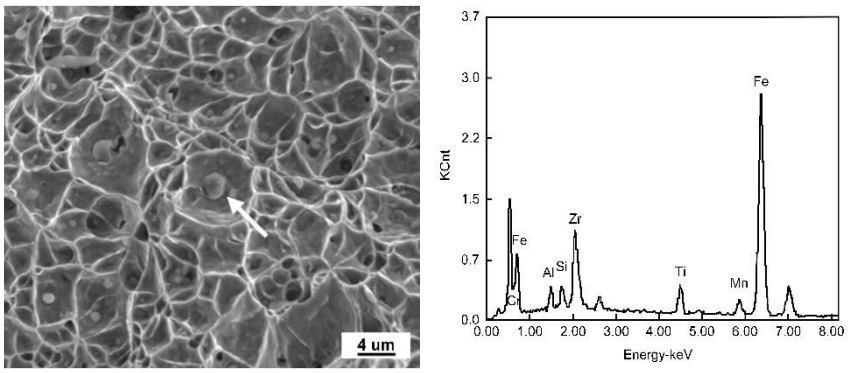

(a) (e)

Preprints (www.preprints.org) | NOT PEER-REVIEWED | Posted: 4 January 2021 doi:10.20944/preprints202101.0064.v1

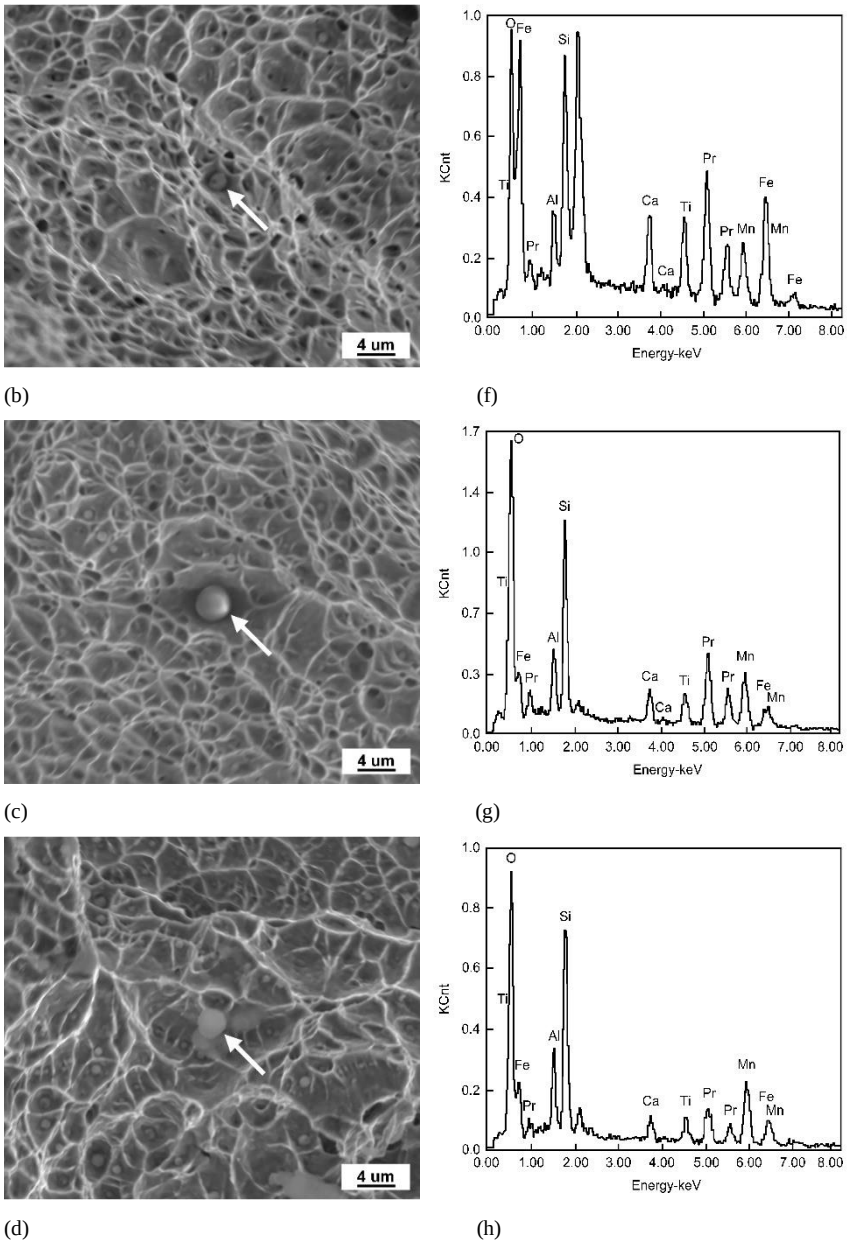

Figure 6. SEM image of inclusion and EDS spectrum in weld metal:
(a) and (e) wire No.1; (b) and (f) wire No.2; (c) and (g) wire No.3; (d) and (h) wire No.4.

When Pr_6O_{11} was not added, the cause of the cracks in the weld metal was the boundary cracking of the B clusters caused by the surface shear stress. The small B cluster size determines the high cleavage fracture stress, which delays the occurrence of cleavage fracture and makes the material have higher impact toughness [20]. Figure 5e and h shows the cleavage fracture caused by the boundary cracking of B clusters, which extended to the critical microfracture surface and through the entire specimen. The control condition for crack growth is: $\sigma y \geq \sigma f$ [21, 22] (σy is the normal stress at the front of the gap, and σf is determined by the size of the critical fracture surface). The crack initiated in the coarsest grain zone, the critical event is the propagation of cracks at the coarsest grains. The cleavage fracture mechanism was different from the ductile fracture mechanism; it did not depend on the density of the second phase particles but on the size of the critical microfracture surface controlled by the phase composition of the microstructure. The coarsest B cluster was the weakest area in the microscopic composition, and the

 doi:10.20944/preprints202101.0064.v1

critical event of cleavage fracture was confirmed as crack propagation through the boundary of the B cluster. The lath structure was refined with high cleavage fracture stress, which delayed the occurrence of cleavage fracture and improved the impact toughness of the material. Figure 5f show the cleavage fracture caused by the decohesion of an inclusion, and the crack initiation was surface shear stress-induced decohesion of the inclusion. The cracks caused by the decohesion of an inclusion of three uninterrupted stages [21]: (1) the dislocations accumulated at the inclusion particles during material deformation, cracks were generated at the interface between the inclusion and the matrix at the end of the dislocation accumulation, (2) the cracks extend through the grain boundary; (3) the grain cracks pass through the grains The boundary expands into adjacent grains. then, the cracks extended through the entire specimen. The addition of an appropriate amount of Pr_6O_{11} in the weld metal promoted the nucleation of inclusions and the formation of AF, which leaded to a change in the fracture mode of the weld metal and improved the impact toughness.

4. Conclusions

(1) With the addition of Pr_6O_{11} from 0% to 3%, the tensile strength, yield strength and hardness of weld metal gradually decreased. The tensile strength ranged from 843 MPa to 809 MPa. The Charpy V-notch impact toughness increased first and then decreased, and the corresponding value was 45 J, 72 J, 61 J, and 46 J, respectively. Wire No.2 with 1% Pr_6O_{11} had the highest toughness and the better strength among the four wires.

(2) The addition of Pr_6O_{11} promoted the formation of rare earth composite inclusions and AF in the weld metal, refined the lath structure, inhibited the formation of M and B, improved the impact toughness of the weld metal. The crack formation mode changed from the boundary cracking of the B clusters caused by the surface shear stress to the surface shear stress-induced decohesion of inclusion. However, excessive addition of Pr_6O_{11} reduced the number of inclusion nucleation and deteriorated the mechanical properties.

(3) The wire No.2 with 1% Pr_6O_{11} had the good comprehensive mechanical properties, and the optimal proportion of microstructure was found in the deposited metal: 60% AF, 8% M, 20% GB, and 12% DUB.

Author Contributions: Conceptualization, T.L.Z.; methodology, T.L.Z. and H.Y.; formal analysis, T.L.Z., H.Y., and S.L.L.; investigation, H.Y., W.W., H.X.C., and Y.C; resources, T.L.Z. and S.L.L.; data curation, T.L.Z. and H.Y.; writing—original draft preparation, T.L.Z. and H.Y.; writing—review and editing, T.L.Z., H.Y., S.L.L, W.G.W., W.W., H.X.C., and Y.C.; visualization, H.Y., S.L.L, and W.G.W.; supervision, T.L.Z.; project administration, T.L.Z.; funding acquisition, T.L.Z. All authors have read and agreed to the published version of the manuscript.

Acknowledgments: This research was funded by National Natural Science Foundation of China (grant No.51804196).

Conflicts of Interest: The authors declare no conflict of interest.

References

1. Ritchie, O.R. The Conflicts between Strength and Toughness. *Nat. Mater.* **2011**, 10, 817-822.
2. Lee, H.W.; Kim, Y. H.; Lee, S. H.; Lee, S. K.; Lee, K. H.; Park, J. U.; Sung, J. H. Effect of Boron Contents on Weldability in High Strength Steel. *J. Mech. Sci. Technol.* **2007**, 21, 771-777.
3. Chai, F.; Yang, C.F.; Su, H.; Zhang, Y.Q. Effect of Zr Addition to Ti-Killed Steel on Inclusion Formation and Microstructural Evolution in Welding Induced Coarse-Grained Heat Affected Zone.

Acta Metall. Sin. **2008**, 21, 220-226.

4. Pouriamanesh, R.; Dehghani, K.; Vallant, R.; Enzinger, Norbert. Effect of Ti Addition on the Microstructure and Mechanical Properties of Weld Metals in HSLA Steels. *J. Mech. Sci. Technol.* **2018**, 27, 6058-6068.
5. Ilman, M.N.; Cochrane, R.C.; Evans, G.M. Effect of Nitrogen and Boron on the Development of Acicular Ferrite in Reheated C-Mn-Ti Steel Weld Metals. *Weld World* **2012**, 56, 41-50.
6. Beidokhti, B.; Koukabi, A.H.; Dolati, A. Effect of Titanium Addition on the Microstructure and Inclusion Formation inSubmerged Arc Welded HSLA Pipeline Steel. *J. Mater. Process. Tech.* **2009**, 209, 4027-4035.
7. Seo, K.; Kim, Y.M.; Kim, H.J.; Lee, C. Characterization of Inclusions Formed in Ti-containing Steel Weld Metals. *ISIJ Int.* **2015**, 55, 1730-1738.
8. Nako, H.; Okazaki, Y.; Speer, J.G. Acicular Ferrite Formation on Ti-Rare Earth Metal-Zr Complex Oxides. *ISIJ Int.* **2015**, 55, 250-256.
9. AWS A5.29/A5.29M: Specification for low-alloy steel electrodes for flux cored arc welding. *American Welding Society* **2005**
10. AWS B4.0: Standard methods for mechanical testing of welds. *American Welding Society* **2007**
11. Liu, Z.; Song, B.; Yang, Z.B.; Cui, X.K.; Li, L.F.; Wang, L.; Song, Z.R. Effect of Cerium Content on the Evolution of Inclusions and Formation of Acicular Ferrite in Ti-Mg-Killed EH36 Steel. *Metals* **2020**, 10, 863.
12. Cai, Y.C.; Liu, R.P.; Wei, Y.H.; Cheng, Z.G. Influence of Y on Microstructures and Mechanical Properties of High Strength Steel Weld Metal. *Mater. Design* **2014**, 62, 83-90.
13. Wan, X.L.; Wang, H.H.; Cheng, L.; Wu, K.M. The Formation Mechanisms of Interlocked Microstructures in Low-Carbon High-Strength Steel Weld Metals. *Mater. Charact.* **2012**, 67, 41-51.
14. Soliman, M. Microstructural Control and Properties Optimization of Microalloyed Pipeline Steel. *Metals* **2020**, 10, 1499.
15. Zhang, T.L.; Li, Z.X.; Young, F., Kim, H.J.; Li H., Jing, H.Y.; Tillmann W. Global Progress on Welding Consumables for HSLA Steel. *ISIJ Int.* **2014**, 54, 1472-1484.
16. Zhang, T.L.; Li, Z.X.; Ma, S.M.; Kou, S.; Jing, H.Y. High Strength Steel (600–900 MPa) Deposited Metals: Microstructure and Mechanical Properties. *Sci. Technol. Weld. Joi.* **2016**, 21, 186-193.
17. Qiu, J.F. The Existing Forms of Rare Earth in the Grain Boundary and Its Influence on the State of the Grain Boundary. *Rare Earth* **1983**, 58-68.
18. Tervo, H.; Kaijalainen, A.; Javaheri, V.; Kolli, S.; Alatarvas, T.; Anttila, S.; Kömi, J. Characterization of Coarse-Grained Heat-Affected Zones in Al and Ti-Deoxidized Offshore Steels. *Metals* **2020**, 10, 1096.
19. Wang, L.J.; Liu, Y.Q.; Wang, Q.; Chou, K.C. Evolution Mechanisms of MgO·Al2O3 Inclusions by Cerium in Spring Steel Used in Fasteners of High-speed Railway. *ISIJ Int.* **2015**, 55, 970-975.
20. Bott, I.S.; Rios, P.R. On the Effectiveness of Inclusions as Nucleation Sites in Weld Deposits. *Scripta Mater.* **1998**, 38, 1269-1274.
21. Chen, J.H.; Cao, R. Micromechanism of Cleavage Fracture of Weld Metals. *Acta Metall. Sin.* **2017**, 53, 1427-1444.
22. Cao, R.; Zhang, X.B.; Wang, Z.; Peng, Y.; Du, W.S.; Tian, Z.L.; Chen, J.H. Investigation of Microstructural Features Determining the Toughness of 980 MPa Bainitic Weld Metal. *Metall. Mater. Trans. A* **2014**, 45, 815-834.